Spin and model identification of Z' bosons at the LHC

P. Osland[*]

Department of Physics and Technology, University of Bergen, Postboks 7803, N-5020 Bergen, Norway

A. A. Pankov[†] and A. V. Tsytrinov[‡]

The Abdus Salam ICTP Affiliated Centre, Technical University of Gomel, 246746 Gomel, Belarus

N. Paver[§]

University of Trieste and INFN-Trieste Section, 34100 Trieste, Italy

Heavy resonances appearing in the clean Drell-Yan channel may be the first new physics to be observed at the proton-proton CERN LHC. If a new resonance is discovered at the LHC as a peak in the dilepton invariant mass distribution, the characterization of its spin and couplings will proceed via measuring production rates and angular distributions of the decay products. We discuss the discrimination of the spin-1 of Z' representative models ($Z'_{\rm SSM}$, Z'_ψ, Z'_η, Z'_χ, $Z'_{\rm LR}$, and $Z'_{\rm ALR}$) against the Randall-Sundrum graviton resonance (spin-2) and a spin-0 resonance (sneutrino) with the same mass and producing the same number of events under the observed peak. To assess the range of the Z' mass where the spin determination can be performed to a given confidence level, we focus on the angular distributions of the Drell-Yan leptons, in particular, we use as a basic observable an angular-integrated center-edge asymmetry, $A_{\rm CE}$. The spin of a heavy Z' gauge boson can be established with $A_{\rm CE}$ up to $M_{Z'} \simeq 3.0$ TeV, for an integrated luminosity of 100 fb^{-1}, or minimal number of events around 110. We also examine the distinguishability of the considered Z' models from one another, once the spin-1 has been established, using the total dilepton production cross section. With some assumption, one might be able to distinguish among these Z' models at 95% C.L. up to $M_{Z'} \simeq 2.1$ TeV.

I. INTRODUCTION

Heavy resonances with mass around 1 TeV or higher are predicted by numerous new physics (NP) scenarios, candidate solutions of conceptual problems of the standard model (SM). In particular, this is the case of models of gravity with extra spatial dimensions, grand unified theories (GUT), electroweak models with extended spontaneously broken gauge symmetry, and supersymmetric (SUSY) theories with R-parity breaking ($\not R_p$). These new heavy objects, or "resonances," with mass $M \gg M_{W,Z}$, may be either produced or exchanged in reactions among SM particles at high energy colliders such as the LHC and the International electron-positron Linear Collider (ILC). A particularly interesting process to be studied in this regard at the LHC is the Drell-Yan (DY) dilepton production ($l = e, \mu$)

$$p + p \rightarrow l^+ l^- + X, \qquad (1.1)$$

where exchanges of the new particles can occur and manifest themselves as peaks in the $(l^+ l^-)$ invariant mass M. Once the heavy resonance is discovered at some $M = M_R$, further analysis is needed to identify the theoretical framework for the NP to which it belongs. Correspondingly, for any NP model, one defines as *identification* reach the upper limit for the resonance mass range where it can be identified as the source of the resonance, against the other, potentially competitor scenarios, that can give a peak with the same mass and same number of events under the peak. This should be compared to the *discovery* reach, which specifies the (naturally more extended) mass range where the peak in the cross section pertaining to the model can just be observed experimentally. Clearly, the determination of the spin of the resonance represents an important aspect of the selection among different classes of non-standard interactions giving rise to the observed peak.

Tests of the spin-2 of the Randall-Sundrum [1] graviton excitation (RS) exchange in the process (1.1) at LHC, against the spin-1 hypothesis, have been recently performed, e.g., in Refs. [2–4] on the basis of the lepton differential polar angle distribution, and in Ref. [5] using the azimuthal angular dependence. In the reverse, the identification of the spin-1 Z's has been discussed in [6,7]. The above-mentioned differential angular analysis in the polar angle has been applied to the search for spin-2,

---
[*]per.osland@ift.uib.no
[†]pankov@ictp.it
[‡]tsytrin@rambler.ru
[§]nello.paver@ts.infn.it

spin-1, and spin-0 exchanges in the experimental studies of process (1.1) at the Fermilab Tevatron proton-antiproton collider [8].

In Ref. [9], the discrimination reach at the LHC on the spin-2 RS graviton resonance or, more precisely, the simultaneous rejection of *both* the spin-1 and spin-0 hypotheses for the peak, has been assessed by using as basic observable an angular-integrated center-edge asymmetry, $A_{\rm CE}$, instead of the "absolute" lepton differential angular distribution. The potential advantages of the asymmetry $A_{\rm CE}$ to discriminate the spin-2 graviton resonance against the spin-1 hypothesis were discussed in Refs. [10,11].

Here, along the lines of Ref. [9] but in the reverse direction, we apply the same basic observable $A_{\rm CE}$, to the spin-1 identification of a peak observed in the dilepton mass distribution of the process (1.1) at the LHC, against the spin-2 and spin-0 alternative hypotheses. For explicit NP realizations, for the spin-1 Z' models we refer to Refs. [12]; for the alternative spin-2 and spin-0 hypotheses we refer for the RS graviton resonance to [1] and for the SUSY $\not{R}_p$ sneutrino exchange to [13,14], respectively.

It turns out that $A_{\rm CE}$ should provide a robust spin diagnostic for the spin-1 case also. Moreover, we examine the possibility, once the spin-1 for the discovered peak is established, of differentiating the various representative Z' models from one another. For this purpose, we must use the total dilepton production cross section or, equivalently, the rate of events of reaction (1.1) under the peak. Identification of Z' models has been discussed recently in, e.g. [7,15,16] with different sets of observables, namely, forward-backward asymmetry $A_{\rm FB}$ on and off the Z' resonance, Z' rapidity distribution, cross section times total width, $\sigma \times \Gamma_{Z'}$, as well as in different processes [17,18]. It was found that, on the basis of $A_{\rm FB}$ only, pairs of Z' models become indistinguishable at a given level of significance, starting from relatively low values of $M_{Z'}$ of the order of 1–2 TeV, even at $\mathcal{L}_{\rm int}$ much higher than 100 fb^{-1}. These ambiguities can be reduced by the combined analysis of the observables mentioned above, and at $\mathcal{L}_{\rm int} =$ 100 fb^{-1}, some models could be discriminated up to Z' mass of the order of 2–2.5 TeV. As we will note below, on the basis of a simple χ^2 criterion, the precise determination of the total cross section itself might provide a somewhat stronger discrimination potential, in the sense that all models could be pairwise distinguished from one another up to Z' masses of about 2.1 TeV.

In Sec. II we present a brief introduction to the main features of the different models considered in the analysis, and the expected relevant statistics; Sec. III is devoted to the spin-1 identification of Z' bosons against the spin-2 RS and the spin-0 sneutrino hypotheses; in Sec. IV we derive the differentiation of Z' models among themselves obtainable at the LHC from consideration of the total dilepton cross sections, whereas Sec. V is devoted to a brief discussion of the reduced-energy, low-luminosity domain

relevant to the early running period of the collider. Finally, Sec. VI contains some conclusive remarks.

II. CROSS SECTIONS AND CONSIDERED NP MODELS

For completeness and to fix the notations, we start by recalling the basic expression for the cross section of process (1.1) and present a mini-review of the NP models we want to compare.

The parton model cross section for inclusive production of a dilepton with invariant mass M can be written as

$$\frac{d\sigma(R_{ll})}{dMdydz} = K\frac{2M}{s}\sum_{ij}f_i(\xi_1, M)f_j(\xi_2, M)$$
$$\times \frac{d\hat{\sigma}}{dz}(i + j \rightarrow l^+ + l^-). \quad (2.1)$$

Here, s is the proton-proton center-of-mass energy squared; $z = \cos\theta_{\rm c.m.}$ with $\theta_{\rm c.m.}$ the lepton-quark angle in the dilepton center-of-mass frame; y is the dilepton rapidity; $f_{i,j}(\xi_{1,2}, M)$ are parton distribution functions in the protons P_1 and P_2, respectively, with $\xi_{1,2} = (M/\sqrt{s}) \times \exp(\pm y)$ the parton fractional momenta; finally, $d\hat{\sigma}_{ij}$ are the partonic differential cross sections. In (2.1), the factor K accounts for next-to-leading order QCD contributions [19,20]. For simplicity, and to make our procedure more transparent, we will use as an approximation a global flat value $K = 1.3$.

Since we are interested in a (narrow) peak production and subsequent decay into the DY pair, $pp \rightarrow R \rightarrow l^+l^-$, we consider the lepton differential angular distribution, integrated over an interval of M around M_R:

$$\frac{d\sigma(R_{ll})}{dz} = \int_{M_R-\Delta M/2}^{M_R+\Delta M/2} dM \int_{-Y}^{Y} \frac{d\sigma}{dMdydz}dy. \quad (2.2)$$

The number of events under the peak, that determines the statistics, is therefore given by

$$\sigma(R_{ll}) \equiv \sigma(pp \rightarrow R) \cdot {\rm BR}(R \rightarrow l^+l^-)$$
$$= \int_{-z_{\rm cut}}^{z_{\rm cut}} dz \int_{M_R-\Delta M/2}^{M_R+\Delta M/2} dM \int_{-Y}^{Y} dy \frac{d\sigma}{dMdydz}. \quad (2.3)$$

For the full final phase space, $z_{\rm cut} = 1$ and $Y = \log(\sqrt{s}/M)$. However, if the finite detector angular acceptance is accounted for, $z_{\rm cut} < 1$ and Y in Eqs. (2.2) and (2.3) must be replaced by a maximum value $y_{\rm max}(z, M)$. Concerning the size of the bin ΔM, it should include a number (at least one) of peak widths to enhance the probability to pick up the resonance. In the models we will consider, widths are predicted to be small, typically of the order of a percent (or less) of the mass M_R, so that the integral under the peak should practically be insensitive to the actual value of ΔM. Conversely, the SM "background" is expected to depend on ΔM. In our analysis, we

adopt the parametrization of ΔM vs M proposed in Ref. [6] and, denoting by N_B and N_S the number of "background" and "signal" events in the bin, the criterion $N_S = 5\sqrt{N_B}$ or 10 events, whichever is larger, as the minimum signal for the peak discovery.

To evaluate the statistics, we shall use in Eqs. (2.2) and (2.3) the CTEQ6.5 parton distributions [21] and impose cuts relevant to the LHC detectors, namely: pseudorapidity $|\eta| < 2.5$ for both leptons assumed massless (this leads to a boost-dependent cut on z [11]); lepton transverse momentum $p_\perp > 20$ GeV. Moreover, the reconstruction efficiency is taken to be 90% for both electrons and muons [22] and throughout this paper, except for Sec. V, a time-integrated LHC luminosity $\mathcal{L}_{\text{int}} = 100$ fb^{-1}.

For the proton-proton initiated process (1.1), only the z-even parts of the partonic differential cross sections contribute to the right side of Eq. (2.2), z-odd terms do not contribute after the y integration.[1] Also, due to $M_Z \ll M_R$ and the narrow-width peak, the resonant amplitude interference with the SM is expected to give negligible contributions to the right-hand sides of (2.2) and (2.3) after the symmetric M integration around M_R needed there. Thus, we can retain in these equations just the SM and the resonance pole contributions.[2] This fact was noticed for Z' exchange in, e.g., Refs. [6,19], but holds also for the RS graviton and for the scalar sneutrino exchanges discussed later.

A. Z' models

In a wide variety of electroweak theories, in particular, those based on extended, spontaneously broken, gauge symmetries, the existence of one (or more) new neutral gauge bosons Z' is envisaged. These additional gauge bosons could be accessible at the LHC. A new neutral gauge boson would induce additional neutral current interactions. The color-averaged differential cross section for the relevant, leading order, partonic subprocess $q\bar{q} \to Z' \to l^+l^-$ can be expressed as[3]

$$\frac{d\hat{\sigma}_{q\bar{q}}^{Z'}}{dz}\bigg|_{z\text{-even}} = \frac{1}{N_c}\frac{\pi\alpha_{\text{em}}^2}{2M^2}[S_q^{Z'}(1+z^2)], \qquad (2.4)$$

with

---

[1]Accordingly, for the $q\bar{q}$ and gg subprocesses, only the combinations of parton distributions $[f_q(\xi_1, M)f_{\bar{q}}(\xi_2, M) + f_{\bar{q}}(\xi_1, M)f_q(\xi_2, M)]$ and $f_g(\xi_1, M)f_g(\xi_2, M)$ are effective in the cross sections (2.2) and (2.3).

[2]Actually, such interference can in principle contribute appreciably to the differential cross section $d\sigma/dMdy$ [9], and plays a role in the forward-backward asymmetry (which we do not consider here).

[3]We neglect fermion masses as well as potential effects from the (tiny) $Z - Z'$ mixing.

$$S_q^{Z'} = \frac{1}{4}((g_L^{q'})^2 + (g_R^{q'})^2)((g_L^{l'})^2 + (g_R^{l'})^2)|\chi_{Z'}|^2,$$

$$\chi_{Z'} = \frac{M^2}{M^2 - M_{Z'}^2 + iM_{Z'}\Gamma_{Z'}}. \qquad (2.5)$$

Equation (2.4) shows that the spin-1, Z', exchange in process (1.1) has the same symmetrical angular dependence as the SM γ and Z exchanges.

The list of Z' models that will be considered in our analysis is the following:

(i) The three possible $U(1)$ Z' scenarios originating from the exceptional group E_6 spontaneous breaking. They are defined in terms of a mixing angle β, and the couplings are as in Table I. The specific values $\beta = 0$, $\beta = \pi/2$, and $\beta = -\arctan\sqrt{5/3}$ correspond to different E_6 breaking patterns and define the popular scenarios Z'_χ, Z'_ψ, and Z'_η, respectively.

(ii) The left-right models, originating from the breaking of an $SO(10)$ grand-unification symmetry, and where the corresponding Z'_{LR} couples to a combination of right-handed and $B - L$ neutral currents (B and L denote lepton and baryon currents), specified by a real parameter α_{LR} bounded by $\sqrt{2/3} \lesssim \alpha_{\text{LR}} \lesssim \sqrt{2}$. Corresponding Z' couplings are reported in Table I. We fix $\alpha_{\text{LR}} = \sqrt{2}$, which corresponds to a pure L-R symmetric model.

(iii) The Z'_{ALR} predicted by the "alternative" left-right scenario.

(iv) The so-called sequential standard model (SSM) Z'_{SSM}, where the couplings to fermions are the same as those of the SM Z.

Detailed descriptions of these models, as well as the specific references, can be found, e.g., in Ref. [12]. All numerical values of the Z' couplings needed in Eq. (2.5) are collected in Table I, where: $A = \cos\beta/2\sqrt{6}$ and $B = \sqrt{10}\sin\beta/12$ are used.

Current Z' mass limits, from the Fermilab Tevatron collider, are in the range 800–1000 GeV, depending on the model [23].

B. RS graviton excitation

We consider the simplest scenario in the class of models based on one compactified warped extra dimension and two branes, proposed in the context of the SM gauge-hierarchy problem in [1]. The model predicts a tower of narrow Kaluza-Klein (KK), spin-2, graviton excitations $G^{(n)}$ ($n \geq 1$) with the peculiar mass spectrum $M^{(n)} = M^{(1)}x_n/x_1$ (x_i are the zeros of the Bessel function, $J_1(x_i) = 0$). Their masses and couplings to the SM particles are proportional to Λ_π and $1/\Lambda_\pi$, respectively, with Λ_π the gravity effective mass scale on the SM brane. For Λ_π of the TeV order, such RS graviton resonances can be exchanged

TABLE I.   Left- and right-handed couplings of the first generation of SM fermions to the Z' gauge bosons, in units of $1/c_W$ for the E_6 and LR models, and $1/s_W c_W \sqrt{1 - 2s_W^2}$ for the ALR model [9], where $c_W = \cos\theta_W$, $s_W = \sin\theta_W$.

Fermions (f)	ν	e	u	d
		E_6 model		
$g_L^{f'}$	$3A + B$	$3A + B$	$-A + B$	$-A + B$
$g_R^{f'}$	0	$A - B$	$A - B$	$-3A - B$
		Left-Right model (LR)		
$g_L^{f'}$	$\frac{1}{2\alpha_{LR}}$	$\frac{1}{2\alpha_{LR}}$	$-\frac{1}{6\alpha_{LR}}$	$-\frac{1}{6\alpha_{LR}}$
$g_R^{f'}$	0	$\frac{1}{2\alpha_{LR}} - \frac{\alpha_{LR}}{2}$	$-\frac{1}{6\alpha_{LR}} + \frac{\alpha_{LR}}{2}$	$-\frac{1}{6\alpha_{LR}} - \frac{\alpha_{LR}}{2}$
		Alternative Left-Right model (ALR)		
$g_L^{f'}$	$-\frac{1}{2} + s_W^2$	$-\frac{1}{2} + s_W^2$	$-\frac{1}{6} s_W^2$	$-\frac{1}{6} s_W^2$
$g_R^{f'}$	0	$-\frac{1}{2} + \frac{3}{2} s_W^2$	$\frac{1}{2} - \frac{7}{6} s_W^2$	$\frac{1}{3} s_W^2$

in the process (1.1) and mimic Z' exchange. The independent parameters of the model can be chosen as the dimensionless ratio $c = k/\bar{M}_{Pl}$ (with k the five-dimensional curvature and $\bar{M}_{Pl} = 1/\sqrt{8\pi G_N}$ the reduced Planck mass), and the mass M_G of the lowest KK resonance $G^{(1)}$. Accordingly, $\Lambda_\pi = M_G/cx_1$.

The differential cross sections for the relevant partonic subprocesses needed in (2.2) and (2.3), $q\bar{q} \rightarrow G \rightarrow l^+ l^-$ and $gg \rightarrow G \rightarrow l^+ l^-$, read, with $\kappa = \sqrt{2}cx_1/M_G$ [2,24–27]

$$\frac{d\hat{\sigma}_{q\bar{q}}^G}{dz} + \frac{d\hat{\sigma}_{gg}^G}{dz} \Bigg|_{z\text{-even}} = \frac{\kappa^4 M^2}{640\pi^2}[\Delta_{q\bar{q}}(z) + \Delta_{gg}(z)]|\chi_G|^2;$$
$$\chi_G = \frac{M^2}{M^2 - M_G^2 + iM_G\Gamma_G}, \qquad (2.6)$$

where

$$\Delta_{q\bar{q}}(z) = \frac{\pi}{8N_c}\frac{5}{8}(1 - 3z^2 + 4z^4),$$
$$\Delta_{gg}(z) = \frac{\pi}{2(N_c^2 - 1)}\frac{5}{8}(1 - z^4). \qquad (2.7)$$

The theoretically "natural" ranges for the RS model parameters are $0.01 \le c \le 0.1$ and $\Lambda_\pi < 10$ TeV [28]. Current lower bounds at 95% C.L. from the Fermilab Tevatron collider are, for the first graviton mass: $M_G > 300$ GeV for $c = 0.01$ and $M_G > 900$ GeV for $c = 0.1$ [23,29].

C. Sneutrino exchange

Sneutrino ($\tilde{\nu}$) exchange can occur in SUSY with R-parity breaking and represents a possible, spin-0, interpretation of a peak in the dilepton invariant mass distribution of the process (1.1). The cross section for the relevant partonic process, $q\bar{q} \rightarrow \tilde{\nu} \rightarrow l^+ l^-$, is flat in z and reads [13]

$$\frac{d\hat{\sigma}_{q\bar{q}}^{\tilde{\nu}}}{dz} = \frac{1}{N_c}\frac{\pi\alpha_{em}^2}{4M^2}\left(\frac{\lambda\lambda'}{e^2}\right)^2|\chi_{\tilde{\nu}}|^2\delta_{qd},$$
$$\chi_{\tilde{\nu}} = \frac{M^2}{M^2 - M_{\tilde{\nu}}^2 + iM_{\tilde{\nu}}\Gamma_{\tilde{\nu}}}. \qquad (2.8)$$

In Eq. (2.8), λ and λ' are the R-parity-violating sneutrino couplings to $l^+ l^-$ and $d\bar{d}$, respectively. Actually, in the narrow-width approximation, the cross section (2.8) turns out to depend on the product $X = (\lambda')^2 B_l$, with B_l the sneutrino leptonic branching ratio. Current limits on X are rather loose [30], and we may consider for this parameter the range $10^{-5} \le X \le 10^{-1}$. For $10^{-4} \le X \le 10^{-2}$, the range is $M_{\tilde{\nu}} \lesssim 280$–800 GeV [23].

D. Statistics and model signature spaces

In Fig. 1, we show the predicted number of resonance (signal) events N_S in the Drell-Yan process (1.1) at LHC, vs M_R, where $R = Z'$, G, $\tilde{\nu}$ denotes the three alternative possibilities outlined in the previous subsections. The assumed integrated luminosity is $\mathcal{L}_{int} = 100$ fb^{-1}, the cuts in phase space relevant to the foreseen detector acceptance specified above have been imposed, and the channels $l = e$, μ have been combined. Also, the minimum signal for resonance discovery above the background at 5σ is represented by the long-dashed line.

For any model, one can define a corresponding *signature space* as the region, in the (M_R, N_S) plot of Fig. 1, that can be "populated" by the model by varying its parameters in the domains mentioned above. Clearly, in regions where the signature spaces overlap, the values of M_R are such that it is not possible to distinguish a model as the source of the peak against the others, because the number of signal events under the peak can be the same. Further analyses are needed in these cases to perform the identification of the peak source. For example, the blue (dark gray) area in Fig. 1 corresponds to the graviton signature space for $0.01 \le c \le 0.1$, while the yellow (light gray) area (which has substantial overlap with the blue one—indicated as

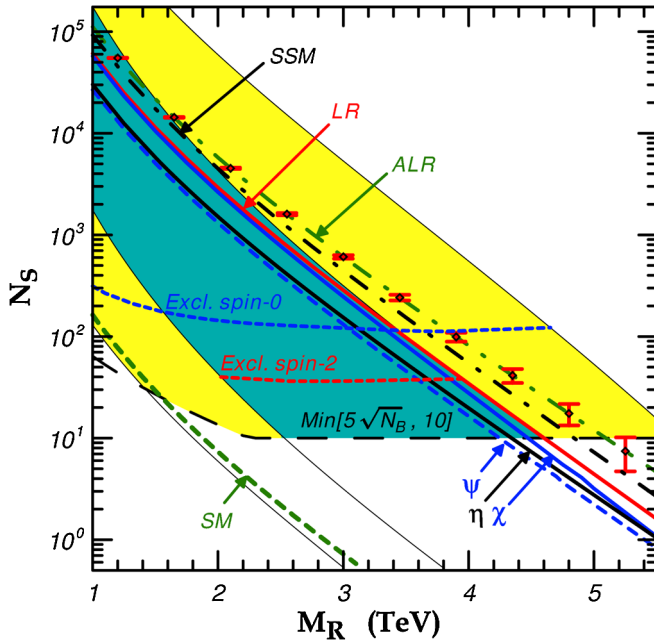FIG. 1 (color online). Expected number of resonance (signal) events N_S vs M_R ($R = Z'$, G, $\tilde{\nu}_\tau$) at the LHC with $\mathcal{L}_{\text{int}} = 100$ fb^{-1} for the process $pp \to R \to l^+ l^- + X$ ($l = e$, μ). Event rates for various Z' models are shown. The green (dark gray) area corresponds to graviton signature space for $0.01 < c < 0.1$ while the yellow (light gray) area is the sneutrino signature space for $10^{-5} < X < 10^{-1}$. The minimum number of signal events needed to detect the resonance (5-σ level) above the background and the minimum number of events to exclude the spin-2 and spin-0 hypotheses at 95% C.L. are shown. Error bars correspond to the statistical uncertainties for the ALR model.

green) is that for the sneutrino signature space corresponding to $10^{-5} \leq X \leq 10^{-1}$.

As regards the discovery and identification of Z' we are interested in, the signature spaces in Fig. 1 reduce to the lines labeled by the different models, because the event rates are fixed, once M'_Z is given, through the couplings in Table I. Figure 1 shows that, with the assumed (high) luminosity of 100 fb^{-1}, Z' gauge boson masses up to 4–5 TeV are in principle within the 5-σ reach of the LHC, consistent with earlier studies [12]. We here assume that the Z' can only decay to pairs of SM fermions in order to obtain the leptonic branching ratio B_l. It is important to note that in many models, where Z' can also decay to exotic fermions and/or SUSY particles, this overestimates B_l and, thus, the search reach.

On the other hand, Fig. 1 demonstrates that, as far as the production rate of DY pairs is concerned, there is a substantial overlap between the Z' and the $\tilde{\nu}$ signature spaces, which determines a domain in $(M_{\tilde{\nu}}, X)$ where spin-0 $\tilde{\nu}$ exchange and Z' exchanges are not distinguishable because they lead to the same event rate under the peak. The same is true for the spin-2, RS model. However, as shown by Fig. 1,

in this case it is interesting to note that, if one literally takes the suggested range $c \lesssim 0.1$ as the "naturally" preferred one, the alternative Left-Right (ALR) and SSM scenarios can be discriminated against the RS (spin-2) resonance *already* at the level of event rates in a wide range of mass values accessible to the LHC, with no need for further analyses. Conversely, only the E_6 and LR Z' models possess a "confusion region" with the RS resonance G, concentrated near the upper border of the graviton signature domain.

III. IDENTIFICATION OF Z' SPIN-1

We now turn to the identification of the spin-1 of the Z' boson vs the spin-0 and spin-2 hypotheses using the angular distribution of the final-state leptons.

For this purpose, we adopt the integrated center-edge asymmetry A_{CE}, defined as [10,11]:

$$A_{\text{CE}}(M_R) = \frac{\sigma_{\text{CE}}(R_{ll})}{\sigma(R_{ll})}, \qquad (3.1)$$

with $\quad \sigma_{\text{CE}}(R_{ll}) \equiv \left[\int_{-z^*}^{z^*} - \left(\int_{-z_{\text{cut}}}^{-z^*} + \int_{z^*}^{z_{\text{cut}}} \right) \right] \frac{d\sigma(R_{ll})}{dz} dz.$

In Eq. (3.1), R denotes the three hypotheses for the resonances we want to compare, namely: spin-1 (V); spin-2 (G); and spin-0 (S). Moreover, $0 < z^* < z_{\text{cut}}$ is an *a priori* free value of $\cos\theta_{\text{cm}}$ that defines the "center" and "edge" angular regions.

Using the differential partonic cross sections reported in the previous sections, one finds the explicit z^* dependencies of A_{CE} for the three cases:

$$A_{\text{CE}}^V \equiv A_{\text{CE}}^{\text{SM}} = \tfrac{1}{2} z^* (z^{*2} + 3) - 1, \qquad (3.2)$$

$$A_{\text{CE}}^G = \epsilon_q^{\text{SM}} A_{\text{CE}}^V + \epsilon_q^G [2z^{*5} + \tfrac{5}{2} z^* (1 - z^{*2}) - 1] + \epsilon_g^G [\tfrac{1}{2} z^* (5 - z^{*4}) - 1], \qquad (3.3)$$

$$A_{\text{CE}}^S = \epsilon_q^{\text{SM}} A_{\text{CE}}^V + \epsilon_q^S (2z^* - 1). \qquad (3.4)$$

In Eq. (3.3), ϵ_q^G, ϵ_g^G, and ϵ_q^{SM} are the fractions of resonant events from the processes $q\bar{q}$, $gg \to G \to l^+ l^-$ and from the SM background, respectively, with $\epsilon_q^G + \epsilon_g^G + \epsilon_q^{\text{SM}} = 1$. Analogous definitions hold for Eq. (3.4), where now $\epsilon_q^S + \epsilon_q^{\text{SM}} = 1$. Their dependence on the dilepton invariant mass M is determined by the overlap of parton distribution functions in Eqs. (2.1) and (2.2). Actually, the above equations strictly hold for $z_{\text{cut}} = 1$, while all the results and figures reported here will be obtained by taking detector cuts into account. Differences turn out to be appreciable and have an impact on the assessment of identification reaches, only near $z^* = 1$, whereas the "optimal" values used in the A_{CE} analysis will be $z^* \approx 0.5$. Thus, Eqs. (3.2), (3.3), and (3.4) are adequate for illustrative purposes, while giving results essentially equivalent to the "full" calculation.

As shown by Eq. (3.2), the peculiar property of the observable $A_{\rm CE}$, as a function of z^*, is that it is the same for *all* spin-1 exchanges, the SM γ, Z, and any Z' model, regardless of the actual values of the left- and right-handed coupling constants to fermions, of the Z' mass $M_{Z'}$ and, to a large extent, of the choice of parton distribution functions. Deviations of $A_{\rm CE}$ from the SM predictions can therefore be attributed to spin-2 or spin-0 exchanges in (1.1).

To assess the domains in which the spin-0 and spin-2 hypotheses can be excluded as sources of a peak observed at $M = M_R$, while giving the same number of events in the assigned interval ΔM in Eq. (2.3), we start from the assumption that spin-1 is the "true" origin of the resonance. The level at which the two alternative hypotheses can be excluded for all "allowed" values of their relevant model parameters is determined by the experimental data, from the prediction of spin-1 (V) exchange, from the predicted spin-0 (S) and spin-2 (G) exchanges, respectively,

$$\Delta A^S_{\rm CE} = A^S_{\rm CE} - A^V_{\rm CE} \quad \text{and} \quad \Delta A^G_{\rm CE} = A^G_{\rm CE} - A^V_{\rm CE}. \quad (3.5)$$

Of course, the identification potential will depend on the available statistics, i.e., from the number of signal events collected in the assigned M interval, in addition to the systematic uncertainties. The latter are however expected to have a reduced influence on $A_{\rm CE}$, because it is a ratio of cross sections.

As an example in Fig. 2, left panel, the center-edge asymmetry $A_{\rm CE}$ is depicted as a function of z^* for resonances with different spins, the same mass $M_R = 3$ TeV,

and the same number N_S of signal events under the peak. As anticipated, the calculations are performed using detector cuts and, also, the SM background has been accounted for. The deviations (3.5) are plotted in the right panel of the figure. The vertical bars attached to the solid line represent, again as an example, the 1-σ statistical uncertainty on the $A^V_{\rm CE}$ corresponding to the Z'_ψ model with the assigned mass $M_{Z'}$. Figure 2 shows that the Z'_ψ model with mass $M_{Z'} = 3$ TeV can be discriminated from the other spin hypotheses at the 2-σ level by means of $A_{\rm CE}$ at $z^* \simeq 0.5$.

While $A^V_{\rm CE}$ is independent of energy, $A^G_{\rm CE}$ and $A^S_{\rm CE}$ are not. In the limit of little background, $\epsilon^{\rm SM}_q$ will be small, and $A^S_{\rm CE}$ will only depend weakly on the energy. On the other hand, even in this limit, $A^G_{\rm CE}$ will in general have a significant dependence on energy, via the relative magnitudes of the fractions ϵ^G_q and ϵ^G_g. An exception to this energy dependence is the region around $z^* \simeq 0.5$, where the coefficient of ϵ^G_q vanishes. In this case, we have

$$A^G_{\rm CE}(z^* \simeq 0.5) > A^S_{\rm CE}(z^* \simeq 0.5). \quad (3.6)$$

This property is of course reproduced in Fig. 2 and allows to conclude that, in order to identify the spin-1 Z' resonance, if one is able to exclude the spin-0 hypothesis, the spin-2 graviton of the RS model will then automatically be excluded.

In order to determine the spin-1 signature space where the spin-0 hypothesis could be excluded against the spin-1 one, the deviation (3.5) should be compared with the
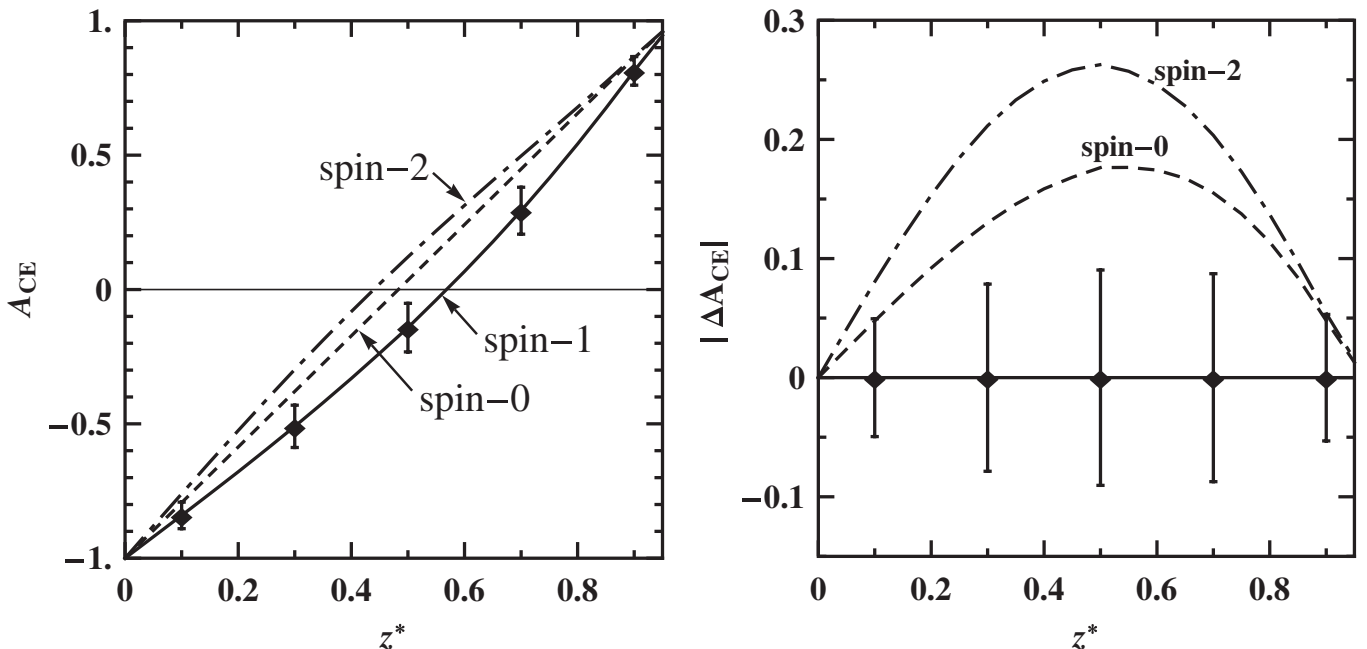

FIG. 2.   Left panel: $A_{\rm CE}$ vs z^* for resonances $\tilde{\nu}$ (spin-0), Z' (spin-1), and G (spin-2) with equal masses of 3 TeV. The error bars are the statistical uncertainties at the 1-σ level on $A^{\rm spin-1}_{\rm CE}$ for the ψ model at 100 fb^{-1}. Right panel: Asymmetry deviations, $|\Delta A_{\rm CE}|$, of the spin-0 and spin-2 hypotheses from the spin-1 one, compared with the uncertainties on $A^{\rm spin-1}_{\rm CE}$.

statistical uncertainty on A_{CE} expressed in terms of the desired number (k) of standard deviations ($k^2 = 3.84$ for 95% C.L.). Notice that in practice A_{CE} is almost unaffected by systematic uncertainty being a relative quantity. We have the condition

$$|\Delta A_{CE}^S| = k \cdot \delta A_{CE}^V, \qquad (3.7)$$

where, taking into account that numerically $(A_{CE}^V)^2 \ll 1$ at $z^* \simeq 0.5$,

$$\delta A_{CE}^V = \sqrt{\frac{1 - (A_{CE}^V)^2}{N_{min}}} \approx \sqrt{\frac{1}{N_{min}}}. \qquad (3.8)$$

From Eqs. (3.7) and (3.8), one therefore obtains

$$N_{min} = N_{min}^S \approx \left(\frac{k}{\epsilon_q^V A_{CE}^V}\right)^2, \qquad (3.9)$$

using the fact that $|A_{CE}^S(z^* \simeq 0.5)|$ is small compared to $|A_{CE}^V(z^* \simeq 0.5)|$, and $\Delta A_{CE}^S = -\epsilon_q^V A_{CE}^V$ with $\epsilon_q^V = 1 - \epsilon_q^{SM} \simeq 1$. From Eq. (3.9) one can easily evaluate the minimal number of events required to exclude the spin-0 hypothesis and, automatically, spin-2 as well, and in this way to establish the spin-1. One finds, using Eq. (3.9) for the exclusion of the spin-0 resonance at 95% C.L., $N_{min} \simeq 110$. One should emphasize that N_{min} determined from Eq. (3.9) is a model-independent value, since A_{CE}^V defined in Eq. (3.2) is independent of specific Z' models, being "universal" for all spin-1 intermediate states. Accordingly, spin-1 of the discovered resonance can be established at 95% C.L. if resonance event samples N_S at the level of N_{min} or larger would be available.

The behavior of N_{min}^S vs M_R, as presented in Fig. 1, is derived from the full calculation including detector cuts, using the general equation (3.7). The intersection of the curves describing N_S against M_R for specific Z' models and displayed in Fig. 1 with the line of N_{min} determines the values of the Z' masses where the spin-1 hypothesis can be identified. One finds that for $M_{Z'} \lesssim 3$ TeV the spin of Z' can be determined at 95% C.L. for all models under study, at 14 TeV, with $\mathcal{L}_{int} = 100$ fb^{-1}. For completeness we also display in Fig. 1 N_{min}^G that lies below N_{min}^S as anticipated.

In addition to the illustrative consideration above, one can quantify the identification reach on the spin-1 hypothesis performing a "conventional" χ^2 analysis to obtain the exclusion domains of the spin-2 and spin-0 hypotheses. In this case, the χ^2 function is defined as

$$\chi^2 = \left[\frac{\Delta A_{CE}}{\delta A_{CE}}\right]^2, \qquad (3.10)$$

with ΔA_{CE} the deviations (3.5) and δA_{CE} the statistical uncertainty (a specific spin-1 Z' model is taken as the true one)
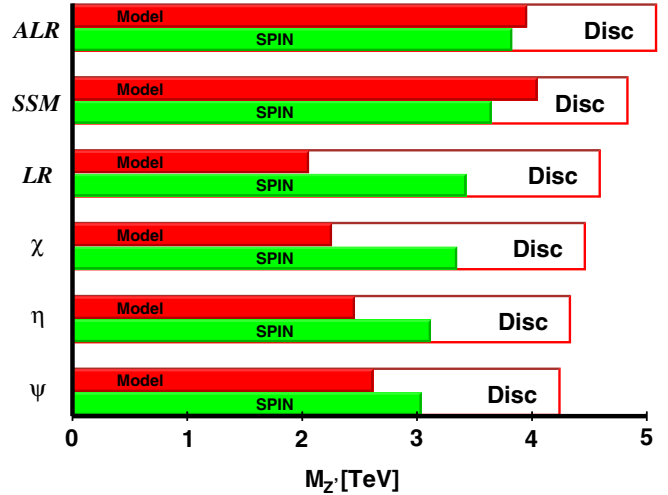

FIG. 3 (color online). Discovery limits on $M_{Z'}$ (5-σ level) and Z'-spin-identification reaches (95% C.L.) for neutral gauge bosons of representative models, using the lepton-pair production cross section $\sigma \cdot B_l$ ($l = e, \mu$) and center-edge asymmetry A_{CE}, respectively, at the LHC with integrated luminosity of 100 fb^{-1}. Also, the Z'-model distinction reaches (95% C.L.) are obtained from the analysis of the leptonic event rates.

$$\delta A_{CE} = \sqrt{\frac{1 - (A_{CE}^V)^2}{\epsilon_l \mathcal{L}_{int} \sigma(V_{ll})}}. \qquad (3.11)$$

Like before, the spin-1 V model can be assumed to be the true one, and the (95% C.L.) exclusion domains of spin-0 and spin-2 can be determined. Here, we combine the channels $l = e, \mu$. The 95% C.L. identification reach of the spin-1 hypothesis in the signature space then results from the domain complementary to the combination of the spin-0 and spin-2 exclusion domains. The results of this numerical analysis are represented in the signature space $(M_{Z'}, N_S)$ in Fig. 1. In fact, the spin-0 exclusion is more restrictive than that for spin-2, as discussed above. Figure 3 gives the "translation" of the discovery reach on Z' models as well as the identification reach on Z' spin presented in Fig. 1, in the form of a histogram. As one can see from Fig. 3, the spin-1 identification (or, actually, the spin-0 and spin-2 exclusion) can be obtained up to Z' mass of the order of 2.5–3.5 TeV, depending on the specific models. The model dependence of the spin-identification reach is due to the difference in statistics, stemming from the different cross sections associated with these models.

It might be useful to conclude this section by emphasizing that the basic observable A_{CE} of Eq. (3.1) only uses the $z = \cos\theta_{c.m.}$ even part of the angular differential distribution, similar to the total cross section. The center and edge angular integration regions are symmetric around $z = 0$ and include events with both signs of z. This might mitigate the impact of the ambiguity, at the pp colliders, in the experimental determination of the sign of z that can affect observables sensitive to the z-odd part of the angular distribution.
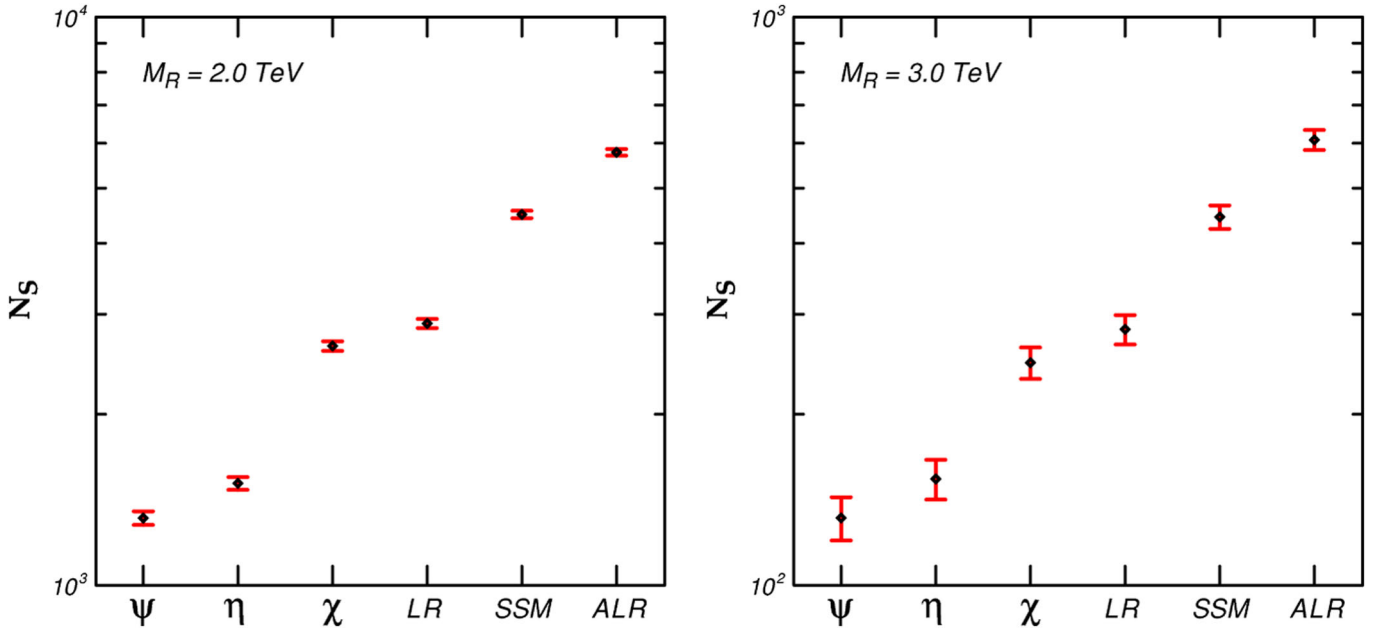
FIG. 4 (color online).   Resonance event rates obtained for the reference models at $M_{Z'} = 2$ TeV (left panel) and 3 TeV (right panel). The error bars show the 1-σ statistical uncertainty at 100 fb^{-1} of integrated luminosity.

IV. DIFFERENTIATING Z' MODELS

Once the spin-1 character of a Z' peak at $M = M_R \equiv M_{Z'}$ has been verified by the exclusion of the spin-0 and spin-2 hypotheses, one can attempt the more ambitious task of identifying the resonance with one of the Z' models by means of the measured production cross section $\sigma \cdot B_l$ or, equivalently, of the peak event rate N_S. As anticipated in Subsection II D, B_l will be assessed under the simplifying assumption of Z' decays to SM fermions only. Results from other observables, such as $\sigma \cdot \Gamma_{Z'}$, A_{FB}, etc., have been qualitatively summarized in Sec. I.[4]

One can see from Fig. 4, representing Z' signal event rates for two specific values of the Z' mass, that at $M_{Z'} = 2$ TeV, an integrated luminosity of 100 fb^{-1} will be sufficient to distinguish all considered models pairwise, whereas at $M_{Z'} = 3$ TeV, one is unable to distinguish neither between Z_ψ vs Z_η nor between Z_χ vs Z_{LR}.

To perform this discrimination, we make the hypothesis that one of the considered models (Z'_{SSM}, Z'_ψ, Z'_η, Z'_χ, Z'_{LR}, or Z'_{ALR}) is the true one, compatible with the measured cross section, and test this assumption against the remaining five models that in general can predict, for the same $M_{Z'}$, a different value of the cross section but within the uncertainty band of the former, hence not distinguishable from it. As a simple criterion, one can define a "separation," in peak event rates N_S, between the true model and the others, and then associate the foreseeable identification reach on the chosen true model to the maximum value of

$M_{Z'}$ for which all five such separations are larger than an amount specified by a desired confidence level. Finally, one can iterate this numerical procedure, in turn, for all six considered Z' models.

For definiteness, we work out explicitly the example of the identification reach on the Z'_{ALR} model. We introduce the relative deviations of the event rates predicted by this model, at the generic $M = M_{Z'}$, from those predicted by the other Z' models:

$$\frac{\Delta N_S}{N_S} = \frac{N_S(Z') - N_S(Z'_{ALR})}{N_S(Z'_{ALR})}. \tag{4.1}$$

Figure 5 shows the relative deviations (4.1) as functions of $M_{Z'}$. Vertical bars represent the 1-σ combination of the statistical uncertainty predicted by the ALR model at integrated LHC luminosity $\mathcal{L}_{int} = 100$ fb^{-1}, with the major systematic uncertainty for the total cross section $\sigma \cdot B_l$, represented by the uncertainties on the parton distribution functions (PDFs). These are calculated using the CTEQ6.5 NLO PDF sets [21].

Corresponding to the definition (4.1), one can introduce a χ^2 function

$$\chi^2 = \left(\frac{\Delta N_S}{\delta N_S}\right)^2 \tag{4.2}$$

with δN_S the corresponding experimental uncertainty, which includes both the statistical and systematic errors combined in quadrature, the former being determined by the Z'_{ALR} model prediction of the event rate. It turns out that for $M \lesssim 4$ TeV the systematic uncertainty is larger than the statistical one, they cross over at a value around 15%. This systematic uncertainty has an effect comparable to
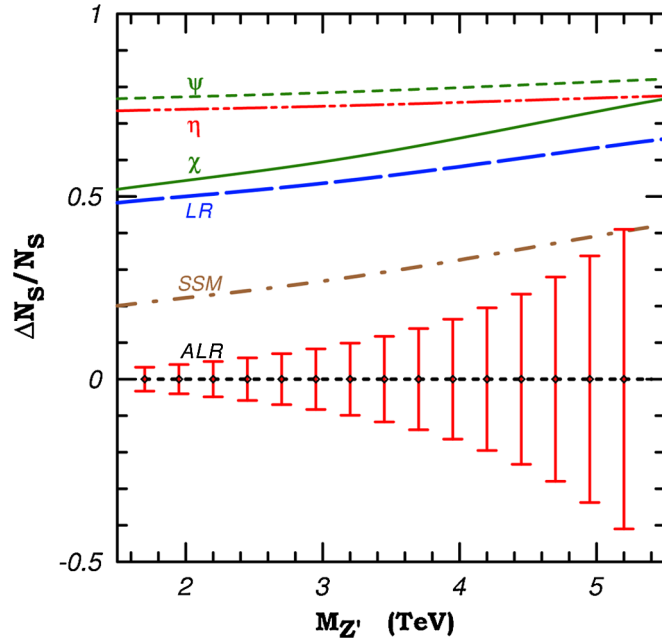
---

[4]Actually, a precise measurement of the ratio $\Gamma_{Z'}/M_{Z'}$, if feasible, might also represent a discrimination criterion among classes of Z' models by itself.

FIG. 5 (color online). Absolute value of relative deviation of the number of events, Eq. (4.1), from the $Z'_{\rm ALR}$ predictions shown in Fig. 1 as a function of $M_{Z'}$ for neutral gauge bosons of representative models. The error bars are the uncertainties at the 1-σ level on $\Delta N_S/N_S$ for the ALR model, $\mathcal{L}_{\rm int} = 100$ fb^{-1}.

that of the statistical uncertainty for Z' resonances with masses larger than 3 TeV [7].

On the basis of such χ^2 we can determine the maximum value of $M_{Z'}$ (hence the identification reach) for which the Z' models, with $Z' \neq Z'_{\rm ALR}$, can be excluded once the ALR model has been assumed to be the true one. This value must satisfy the conditions $\chi^2 > \chi^2_{\rm C.L.}$ for all Z's, where $\chi^2_{\rm C.L.}$ determines the chosen confidence level. The results of this procedure, applied in turn to all six Z' models, are reported in Fig. 3, together with the discovery and the spin-1 identification reaches, and indicate that all models under consideration might be distinguishable up to M'_Z of the order of 2.1 TeV.

Of course, these results rely numerically on the assumption about Z' decay stated at the beginning. On the other hand, neither of the Z' curves in Fig. 1 intersects with any other, so that the simple (and directly measurable) total cross section might also be considered a natural discriminator among models.

V. THE REDUCED-ENERGY, LOW-LUMINOSITY CASE

It may take quite some time before the experiments will be able to collect 100 fb^{-1} of data at 14 TeV. In the present section, we indicate how the spin-identification reach depends on the integrated luminosity, at two different energies, 10 and 14 TeV. The former is expected to be the energy initially available at the LHC.

Of course, in general, a detailed assessment of the spin-identification dependence vs the total energy and the Z' mass depends on the, in some cases complicated behavior of the individual parton distribution function, in addition to the applied cuts. Nevertheless, for a simplified estimate leading to an explicit, parametric, expression of such energy dependence, in a very rough sense one can trade energy for luminosity. Indeed, according to Sec. III, the procedure of Z' spin-1 determination using $A_{\rm CE}$ basically consists in excluding the spin-0 case, since spin-2 is then automatically excluded. The spin-0 cross section is determined by the parton cross section together with the overlap of the d and $\bar{d}$ parton distribution functions in the proton,

$$I_{d\bar{d}}(s, M) = \int dy f_d(\xi_1, M) f_{\bar{d}}(\xi_2, M). \quad (5.1)$$

The spin-1 cross section also depends on the corresponding overlap of the u and $\bar{u}$ parton distribution functions, $I_{u\bar{u}}(s, M)$. In the approximation that these two overlap integrals have the same dependence on $E = \sqrt{s}$, and in the narrow-width approximation, all these cross sections would have the same energy dependence, but they would differ by constant ratios. Thus, the spin-identification reach would be proportional to a unique function of energy, or equivalently, integrated luminosity, the same function for all Z' models. This reach would be given by the number of events, proportional to the integrated luminosity, the parton cross section $\hat{\sigma}$, and the overlap integral:

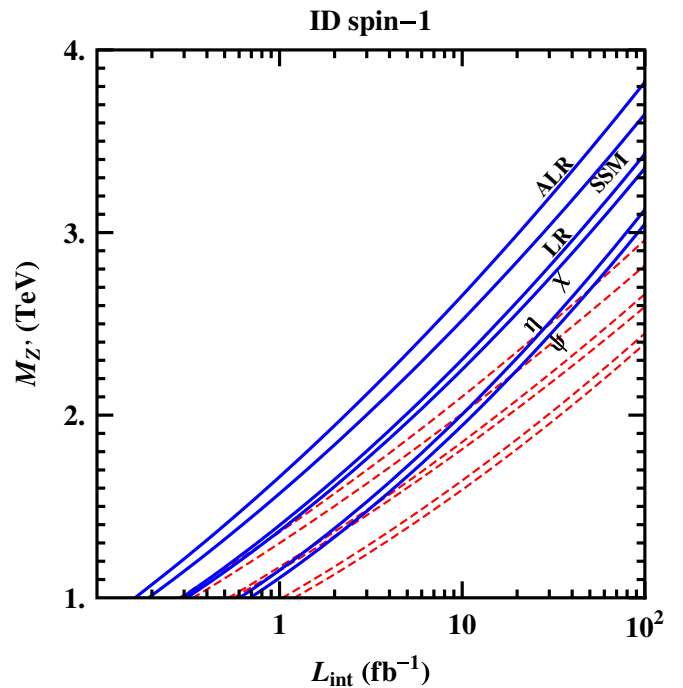$$N \sim \mathcal{L}_{\rm int} \hat{\sigma} I(s, M). \quad (5.2)$$

FIG. 6 (color online). Spin-determination reach as a function of integrated luminosity, for 10 TeV (dashed lines) and 14 TeV (solid lines).

The spin-identification reach basically requires a certain number of events (around 110 at the higher values of $M_{Z'}$), i.e., the scaling with energy and luminosity is determined by keeping the above expression fixed as the luminosity or energy is changed. In the exponential approximation to the overlap integral, given by Eq. (3.16) of Leike [12] (valid for a wide range of $E/M_{Z'}$), this becomes

$$N \sim \mathcal{L}_{\text{int}} \frac{C_1}{E^2} \exp\left[-\frac{C_2 M_{Z'}}{E}\right]. \qquad (5.3)$$

Neglecting the energy and mass dependences of C_1 and C_2, one finds a reach in $M_{Z'}$ that grows linearly with $\log \mathcal{L}_{\text{int}}$, with a slope proportional to the beam energy, features which are qualitatively reflected in Fig. 6, which displays the spin-1 identification reach vs the Z' mass for the various models at the two energies mentioned above. Experimental cuts have been taken the same as detailed in Sec. II for both cases.

Figure 6 speaks for itself. It shows that at 10 TeV, and depending on the model, with a considerable fraction of 1 fb^{-1} one could in principle identify the spin-1 of a hypothetical Z' with mass in the range 1–1.5 TeV. This range is expected to be in the reach of the Tevatron, for the planned luminosity increase from 2.5 up to 9 fb^{-1} [23]. However, the spin identification would be a unique feature of the LHC.

VI. SUMMARY

We can summarize the main part of this paper, relevant to the Z' identification at 14 TeV and 100 fb^{-1} luminosity, as follows: if new heavy resonance peaks will be discovered in the dilepton mass distributions for process (1.1), a Z' can be observed up to $M_{Z'} \approx 4$–5 TeV. The statistical significance of measurements of the evenly integrated (in $\cos\theta_{\text{c.m.}}$) asymmetry A_{CE} will allow to establish the spin-1 (or, to exclude the spin-0 and spin-2) of a heavy Z' gauge boson for $M_{Z'} \lesssim 3.0$–3.8 TeV, at 95% C.L. We also assess the mass limits on Z' for which the studied Z' models can be distinguished, besides their common spin-1, in pairwise comparisons with each other. By a simple criterion based on the expected statistics, we find that with 100 fb^{-1} of integrated luminosity one should be able to distinguish among the six Z' models up to $M_{Z'} \simeq 2.1$ TeV (95% C.L.).

ACKNOWLEDGMENTS

[1] L. Randall and R. Sundrum, Phys. Rev. Lett. **83**, 3370 (1999); **83**, 4690 (1999).

[2] B. C. Allanach, K. Odagiri, M. A. Parker, and B. R. Webber, J. High Energy Phys. 09 (2000) 019.

[3] B. C. Allanach, K. Odagiri, M. J. Palmer, M. A. Parker, A. Sabetfakhri, and B. R. Webber, J. High Energy Phys. 12 (2002) 039.

[4] R. Cousins, J. Mumford, J. Tucker, and V. Valuev, J. High Energy Phys. 11 (2005) 046.

[5] H. Murayama and V. Rentala, arXiv:0904.4561.

[6] D. Feldman, Z. Liu, and P. Nath, J. High Energy Phys. 11 (2006) 007.

[7] F. Petriello and S. Quackenbush, Phys. Rev. D **77**, 115004 (2008).

[8] A. Abulencia *et al.* (CDF Collaboration), Phys. Rev. Lett. **95**, 252001 (2005).

[9] P. Osland, A. A. Pankov, N. Paver, and A. V. Tsytrinov, Phys. Rev. D **78**, 035008 (2008).

[10] P. Osland, A. A. Pankov, and N. Paver, Phys. Rev. D **68**, 015007 (2003).

[11] E. W. Dvergsnes, P. Osland, A. A. Pankov, and N. Paver, Phys. Rev. D **69**, 115001 (2004).

[12] For reviews see, e.g.: J. L. Hewett and T. G. Rizzo, Phys. Rep. **183**, 193 (1989); A. Leike, Phys. Rep. **317**, 143 (1999); T. G. Rizzo, arXiv:hep-ph/0610104; P. Langacker, arXiv:0801.1345.

[13] J. Kalinowski, R. Ruckl, H. Spiesberger, and P. M. Zerwas, Phys. Lett. B **406**, 314 (1997); **414**, 297 (1997); T. G. Rizzo, Phys. Rev. D **59**, 113004 (1999). For a review see, e.g.: R. Barbier *et al.*, Phys. Rep. **420**, 1 (2005).

[14] B. Allanach *et al.* (R parity Working Group Collaboration), arXiv:hep-ph/9906224.

[15] M. Dittmar, A. S. Nicollerat, and A. Djouadi, Phys. Lett. B **583**, 111 (2004).

[16] R. Cousins, J. Mumford, and V. Valuev, Report No. CERN-CMS-NOTE-2005-022, 2005.

[17] S. Godfrey, P. Kalyniak, and A. Tomkins, in *Proceedings of the 2005 International Linear Collider Physics and Detector Workshop, Snowmass, Colorado, 2005*, econf C0508141, ALCPG0108 (2005).

[18] S. Godfrey and T. A. W. Martin, Phys. Rev. Lett. **101**, 151803 (2008).

[19] M. S. Carena, A. Daleo, B. A. Dobrescu, and T. M. P. Tait, Phys. Rev. D **70**, 093009 (2004).

[20] P. Mathews, V. Ravindran, K. Sridhar, and W. L. van Neerven, Nucl. Phys. **B713**, 333 (2005); P. Mathews, V. Ravindran, and K. Sridhar, J. High Energy Phys. 10 (2005) 031; P. Mathews and V. Ravindran, Nucl. Phys. **B753**, 1 (2006); M. C. Kumar, P. Mathews, and V. Ravindran, Eur. Phys. J. C **49**, 599 (2007); D. Choudhury, S. Majhi, and V. Ravindran, Nucl. Phys. **B660**, 343 (2003).

[21] J. Pumplin, D. R. Stump, J. Huston, H. L. Lai, P. Nadolsky,

and W. K. Tung, J. High Energy Phys. 07 (**2002**) 012.

[22] *Proceedings of the Conference "Physics at LHC," Vienna, Austria, 2004*, edited by M. Finger, A. Janata, and M. Virius [Czech. J. Phys. 55, 651 (2005)].

[23] T. Aaltonen *et al.* (CDF Collaboration), Phys. Rev. Lett. **99**, 171802 (2007); **102**, 091805 (2009); R. J. Hooper (D0 Collaboration), Int. J. Mod. Phys. A **20**, 3277 (2005).

[24] T. Han, J. D. Lykken, and R. J. Zhang, Phys. Rev. D **59**, 105006 (1999).

[25] G. F. Giudice, R. Rattazzi, and J. D. Wells, Nucl. Phys. **B544**, 3 (1999).

[26] J. Bijnens, P. Eerola, M. Maul, A. Mansson, and T. Sjostrand, Phys. Lett. B **503**, 341 (2001).

[27] E. Dvergsnes, P. Osland, and N. Ozturk, Phys. Rev. D **67**, 074003 (2003); T. Buanes, E. W. Dvergsnes, and P. Osland, Eur. Phys. J. C **35**, 555 (2004).

[28] H. Davoudiasl, J. L. Hewett, and T. G. Rizzo, Phys. Rev. Lett. **84**, 2080 (2000); Phys. Rev. D **63**, 075004 (2001).

[29] V. M. Abazov *et al.* (D0 Collaboration), Phys. Rev. Lett. **100**, 091802 (2008).

[30] For a review of experimental constraints on *R*-violating operators, see: G. Bhattacharyya, arXiv:hep-ph/9709395; Nucl. Phys. B, Proc. Suppl. **52A**, 83 (1997); H. K. Dreiner, *Perspectives on Supersymmetry*, edited by G. Kane (World Scientific, Singapore, 1998); B. C. Allanach, A. Dedes, and H. K. Dreiner, Phys. Rev. D **60**, 075014 (1999).